



HAL
open science

Turbulence in real flammable gas releases

Didier Jamois, Christophe Proust, Jérôme Hebrard, Emmanuel Leprette, Helene Hisken, Lorenzo Mauri, Gordon Atanga, Melodia Lucas, Kees van Wingerden, Trygve Skjold, et al.

► **To cite this version:**

Didier Jamois, Christophe Proust, Jérôme Hebrard, Emmanuel Leprette, Helene Hisken, et al.. Turbulence in real flammable gas releases. 13th International symposium on hazards, prevention, and mitigation of industrial explosions (ISHPMIE), Jul 2020, Braunschweig, Germany. ineris-03319937

HAL Id: ineris-03319937

<https://ineris.hal.science/ineris-03319937>

Submitted on 13 Aug 2021

HAL is a multi-disciplinary open access archive for the deposit and dissemination of scientific research documents, whether they are published or not. The documents may come from teaching and research institutions in France or abroad, or from public or private research centers.

L'archive ouverte pluridisciplinaire **HAL**, est destinée au dépôt et à la diffusion de documents scientifiques de niveau recherche, publiés ou non, émanant des établissements d'enseignement et de recherche français ou étrangers, des laboratoires publics ou privés.

Turbulence in real flammable gas releases

Didier Jamois^a, Christophe Proust^a, Jérôme Hébrard^a, Emmanuel Leprette^a, Helene Hisken^b, Lorenzo Mauri^b, Gordon Atanga^b, Melodia Lucas^b, Kees van Wingerden^b, Trygve Skjold^c, Pierre Quillatre^d, Antoine Dutertre^e, Thibault Marteau^e, Andrzej Pekalski^f, Lorraine Jenney^g, Dan Allason^g, & Mike Johnson^g

^a Ineris, Verneuil-en-Halatte, France

^b Gexcon R&D, Bergen, Norway

^c University of Bergen, Norway

^d GRTgaz, Safety and Risk Assessment, France

^e Total, France

^f Shell Global Solutions, UK

^g DNV GL Spadeadam Testing and Research, UK

E-mail: didier.jamois@ineris.fr

Abstract

The research activities in AIRRE project (Assessing the Influence of Real Releases on Explosions) include a unique series of large-scale explosion experiments with ignited high-momentum jet releases of natural gas directed into congested geometries. The primary objective for the AIRRE project is to gain improved understanding of the effect realistic releases and turbulent flow conditions have on the course and consequences of accidental gas explosions in the petroleum industry, and thereby develop and commercialize technology and methodology that can facilitate safe and optimal design of process facilities.

A few tests were performed in open air without any congestion. The mean velocity and turbulence flow fields are presented herein. Flameproof turbulence sensors were purposely designed for the project and calibrated at small scale. These are Pitot probes connected to fast differential pressure sensors. This paper describes the turbulence measurement technique used and highlights the specific issues related to the data post-processing in order to calculate the turbulence intensity and the turbulent length scale. Test results are analysed, and comparisons are made with free jet experiments at small scale, and related jet theories.

Keywords : *realistic releases, large-scale experiments, gas explosions, turbulence*

1. Introduction

Accidental releases of pressurized combustible gas in congested industrial environments generate flammable fuel air clouds with high levels of turbulence. The current practice for estimating the consequences of accidental explosions, for instance as part of quantitative risk assessments, entails the use of the so-called equivalent gas cloud method (Hansen *et al.*, 2013). However, the available concepts for defining equivalent gas clouds do not account for the combined effect of pre-ignition turbulence and explosion-generated turbulence on explosion pressures and critical separation distances. Furthermore, there are very limited data available in the public domain for validating consequence models that describe such scenarios. This may result in either severe over-prediction or severe under-prediction of the consequences of explosions.

Following a detailed review of previous experimental work on the effect of realistic releases on explosions (Skjold *et al.*, 2018), primary objective for the AIRRE project (Assessing the Influence of Real Releases on Explosions) is to gain improved understanding of the effect realistic releases and turbulent flow conditions have on the course and consequences of accidental gas explosions. The

experimental program includes a set of tests that investigate the influence of pre-ignition turbulence generated by high-momentum releases on explosion effects and critical separation distances. The goal is to reduce the uncertainty in the estimation of consequences for accidental explosions by developing and validating more accurate models for the physical phenomena involved, in conjunction with improved methodology.

Even if turbulence has been a field of investigation for decades with an important amount of experimental results obtained at lab scale, to our knowledge very few data have been obtained at the industrial scale. This lack was partially filled during AIRRE program. The present work focusses on large free releases performed in open air, equipped with a specific turbulence instrumentation. The specific issues related to the instrumentation and to the data post-processing in order to calculate the turbulence intensity, the turbulent length scale and flow field are described hereafter.

2. Experimental conditions

2.1 Hardware

DNV GL Spadeadam Research and Testing conducted the large-scale experimental campaign in AIRRE project in the Spadeadam test site (UK).

The releases were produced from blowing down a storage reservoir containing approximately 22 Tons of natural gas when charged to its operating pressure of 150 barg. When depleted from 150 barg to 90 barg through a 100 mm orifice, the amount of natural gas expelled is approximately 10 Tons in 100 s meaning 100 kg/s release rate. The release point was flowing horizontally 1.5 m above the ground over a flat area measuring approximately 70 m by 320 m. The releases were oriented along the 320 m axis of the test area (figure 1).

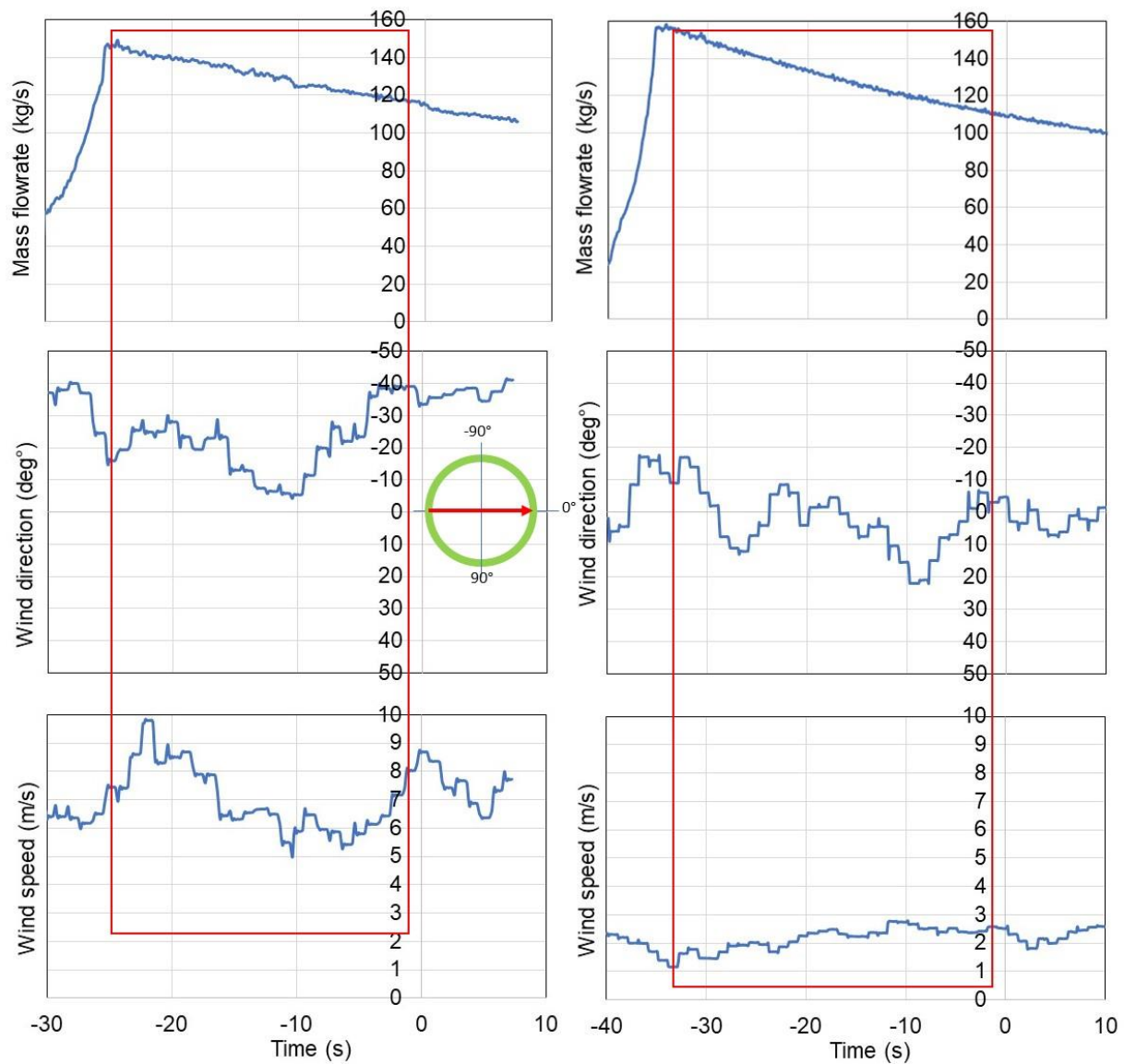


Fig. 1. AIRRE Experimental area on SPADEADAM test site

2.2 Test conditions

The AIRRE campaign included 16 tests. Three tests with un-obstructed jet (tests n°1, 2 and 15), and the rest with obstacles located in the central part of the jet. The focus is on the un-obstructed jets, and particularly on test n°2 and 15 for which turbulent data were recorded.

As shown on figure 2 (mass flowrate curves), the jet is allowed to settle for about 30 seconds before ignition (time 0). It takes about 10 seconds for the jet to reach a steady state, knowing that the pressure in the vessel is decreasing from about 120 bar down to about 90 bar at ignition. In the meantime, outside conditions (wind velocity and wind direction) may vary.



...

Fig. 2. Mass flow rate and wind conditions during the free jet releases n°2 (left) and 15 (right). Red frames indicate the time window used to process the release data

2.3 Probes distribution

As shown by Kristen *et al.* (2020), various categories of probes were used: up to 20 pressure transducers, 20 ionisation probes, fluxmeters... and about 20 velocity probes. Only the latter are considered in this paper. The layout is shown on Figure 3. Turbulent probe signals are recorded at a rate of 500 kHz during the entire duration of the release, but only the most stable part of these records is exploited (red frames in figure 2).

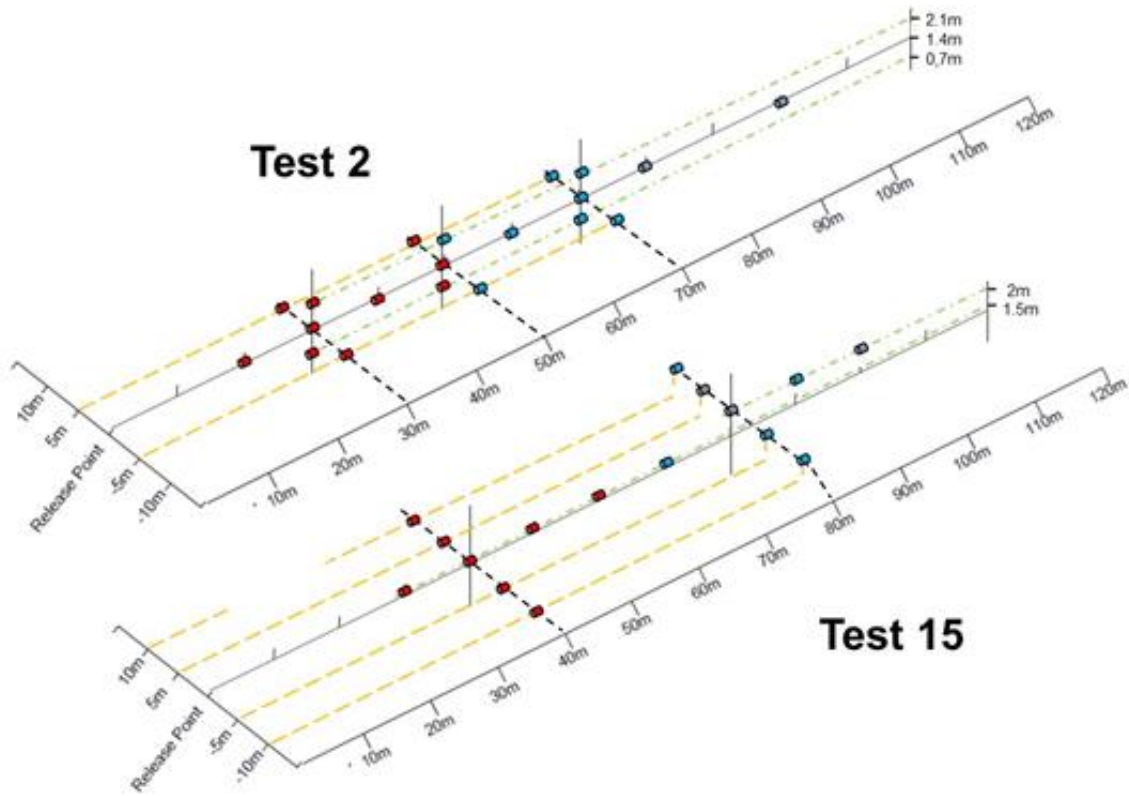


Fig. 3. turbulent probe layout for the two free jet releases studied. Red symbol corresponds to large range sensors (± 7000 Pa) and blue one to lower range sensors (± 1250 Pa)

Some information about the performances of the probes and about the expected behaviour of the kind of jet produced in AIRRE are given in the next section.

3. Measuring the aerodynamics in the jet

3.1 Bidirectional probes

Experience shows that it may prove difficult to use standard laboratory techniques (LDA, PIV, hot wire) in real scale conditions, especially the one produced in AIRRE where even stone were lifted by the momentum of the jet!

Following the pioneering work of Tamanini (Tamanini, 1990, 1991), the original Mc Caffrey technique (Mc Caffrey, 1976) was progressively adapted to the measurement of the turbulence in such situations. The Mc Caffrey gauge is based on the Pitot tube technique (differential pressure measurement). The ability to measure turbulence with this technique is dependent on the features of the differential pressure sensor used and the way it is mounted to the probe. The gauge (Fig.4) is a head connected via small tube to a differential pressure sensor. The head is a tube facing the flow with a wall in the middle, the pressure difference on both sides of the wall is measured and is close to the dynamic pressure of the flow.

The relevant theory and the performances are detailed elsewhere (Proust *et al.*, 2020). For the present purpose, it should be said that the bidirectional probe measures the modulus of the mean velocity and the fluctuations along the axis of the probe. The cutoff frequency is almost 200 Hz (reported value from the supplier) and the measuring range is 1 m/s to 100 m/s.

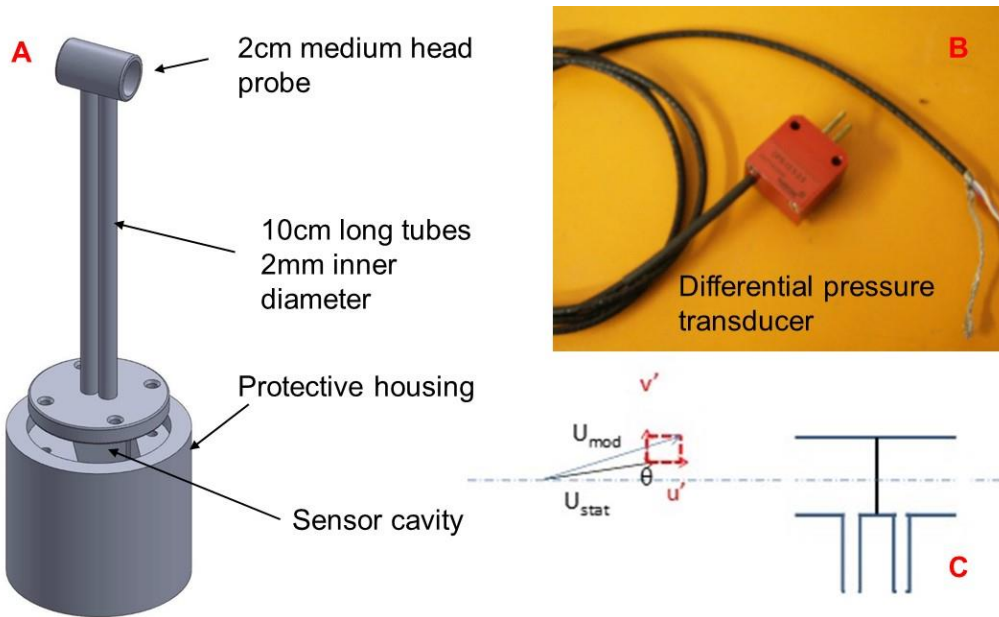


Fig. 4. A : Drawing of the turbulent probe designed for AIRRE with B : the transducer used. C : U_{mod} is the instantaneous modulus of the velocity vector and U_{stat} is the average of the velocity field as defined in the Reynolds approximation. u' and v' are the velocity fluctuations along the axis of the probe and in the radial direction.

An example of the performance of this probe is shown on figure 5. The configuration is a free round subsonic jet of air in the open atmosphere and the measurement is performed on the axis of the jet. The instantaneous velocity is extracted from the dynamic pressure, the mean velocity is the time average and the fluctuations are the difference between the instantaneous velocity and the mean one. The space correlation $R(x)$ is approximated using the time autocorrelation curve and the Taylor assumption ($R(x) = R(t) \cdot \bar{U}$).

Given the intensity of the velocity fluctuations this can only be a rough approximation. From this correlation curve the integral scale of the turbulence is derived using the theoretical relation:

$$L_{int} = \int_0^{+\infty} R(x) \cdot dx$$

Using the same correlation curve, the “spectral energy” of the turbulence may be obtained using:

$$E(\kappa) = \frac{2}{\pi} \cdot u'^2 \cdot \int_0^{\infty} R(x) \cdot \cos(\kappa \cdot x) \cdot dx$$

The spectral energy $E(\kappa)$ (units m^3/s^2) is the kinetic energy per unit mass and per unit wavenumber of fluctuations around the wavenumber κ ($\kappa = 2\pi/\lambda$, where λ is the wavelength/size of the eddies). The spectral energy describes the turbulent cascade of a flow and depends on the former parameters u' and L_{int} (Hinze, 1975).

Under the present experimental conditions, the theoretical and measured jet correlations and turbulence spectrum are shown on figure 5. The agreement seems reasonable.

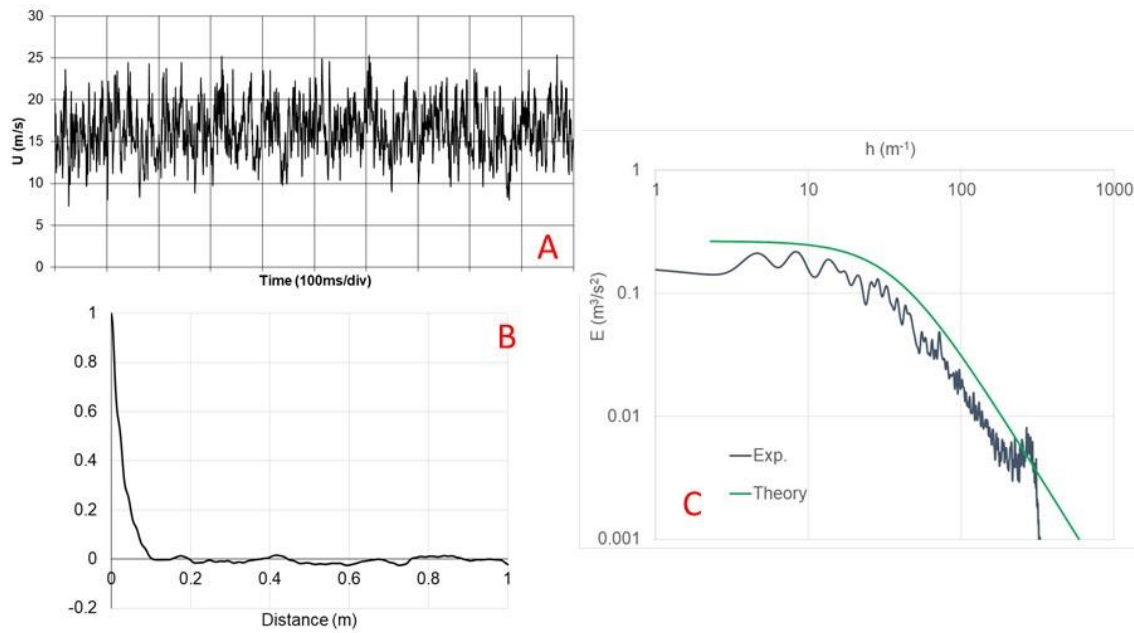


Fig. 5. A: Velocity raw data. B: Autocorrelation curve $R(x)$ obtained from A. C: Spectral Energy as the Direct Fourier Transform from $R(x)$. The green solid curve represents the theoretical expression of $E(\kappa)$ for high Reynolds flow following Hinze

3.2 “Crawling” jet

Large accidental releases have little chance to be round free jets. They rather may be impinging jets, jets in congested zone or “crawling” jets. The latter, which corresponds to the AIRRE configuration investigated in this paper, may be assimilated to the “wall jet theory” which has been studied due to engineering applications such as inlet devices in ventilation, separation control on airfoils and film-cooling of turbine blades (among others: Launder *et al.*- 1983, Hussein *et al.* - 1994, Abrahamsson *et al.*-1996, Sun - 2002, Khritov *et al.*- 2002)

The typical “wall jet” is a turbulent round jet exiting over a flat plate and parallel to it. Investigations have shown that the mean velocity and turbulent stress profiles are self-similar in the far field. The main feature is that the spreading rate parallel to the wall is 5 to 7 time greater than the spreading rate normal to the wall. The mainstream velocity (along x) in the far field is poorly documented and frequently assimilated to that of the free jet. In the near field (up to $50/D$, D being the notional release diameter) correlations based on experimental results were proposed by Sun and Khritov.

The experimental program EXJET (INERIS, 2014-2016) aimed to study at a relatively large scale (about 1 kg/s) the physical mechanism of explosion in a flammable jet. The bidirectional probes were used to measure the velocity and the turbulence in the jet prior to ignition (figure 6). Different industrial accidental situations were simulated and in particular the free crawling jet. It was highlighted that the mainstream velocity obeys a self-similar profile and that the turbulence intensity conforms with the free jet theory along the axis.



Fig. 6. View of an EXJET crawling jet (release diameter: 12mm, flowrate about 1 kg/s)

It can be convenient to assimilate a crawling jet to a half free jet (or a half cone) neglecting the friction at the wall. It is equivalent to calculate velocity and turbulence profiles along the jet axis using a flowrate twice that of the real crawling jet. This effect would increase the size of the jet. But in reality the presence of the wall increases sharply the lateral spreading (and mixing) as compared to a round free jet so that both effects more or less compensate as noticed by Khritov et al.. These authors suggest that the round free jet correlation might provide a reasonable approximation of the crawling jet properties, along the axis (at least $(U_{max}/U_{exit} = 5.8/(x/D - 4.25))$ for the velocity).

Figure 7 gives an example of velocity measurement along x axis for a crawling jet of methane from an orifice of 12mm located 20cm above the ground and an upstream pressure of 40 bar. On fig. 7, the correlations of Sun and Abrahamsson are indicated (respectively the red and green diamonds) together with the self-similar correlation based on the round free jet correlation (solid orange line). The exit velocity (U_{exit}) is set at 400m/s in this case (sound speed) and the notional diameter D is 42mm (Birch -1984 theory, with a discharge coefficient = 1).

There is a reasonable agreement between the various wall jet correlations and the present data points from EXJET experimental series.

A gap appears between the wall jet near field correlation (Sun) and the EXJET data from about 30 x/D . Since the wall jet experiments conducted by Sun were performed with a release velocity rate of about 40m/s, the results are suspected to be unreliable because lying in the lower range of the instrument (hot wire device in that case).

The turbulence intensity from EXJET is in reasonable agreement with the wall jet correlation for values of x/D between 100 and about 200. Above 200, the means jet velocity is comparable to that of the surrounding atmosphere and the plume may not be aligned with the jet axis anymore (the local axial velocity U drops whereas u' remains constant so that u'/U increases). For x/D below 100, the velocity fluctuations are too fast to be captured by the probe.

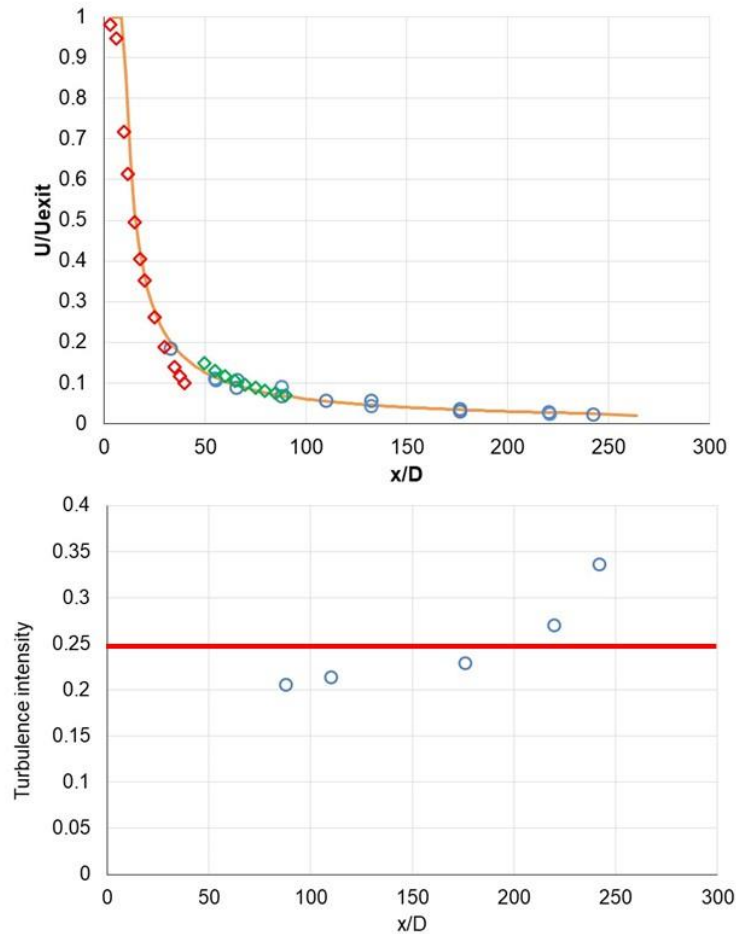


Fig. 7. Upper diagram - Exjet velocity results for a methane crawling jet (blue circle) together with H. Sun correlation (red diamonds), H. Abrahamsson correlation (green diamonds) and round free jet model (solid curve). Bottom diagram – Measured turbulence intensity along the x axis for the same release

The free releases studied in AIRRE project can clearly be considered as crawling jets (figure 1). It then may be interesting to compare the velocity measurement to the correlations cited above.

4. Results

4.1 Data selection

AIRRE real scale conditions were particularly harsh since the momentum was so large that even stones were lifted away down to about 50 to 70 m from the release. Often, the measuring masts were impacted and sometimes thrown away. Furthermore, the videos clearly show that an important quantity of dust/mud is raised and blown away until a steady state is reached.

under such circumstances, it is not surprising to find that many of probes were suspected to be clogged with dust and mist, misaligned or even destroyed.

One particularly tricky work was to sort out unreliable data. To do that each raw record was studied, and only realistic ones were selected (uncapped raw data, steady on average, for about 20 seconds, without any disruption or baseline shift). Only about 30% of the probes gave reliable results for tests n°2 and 15. The labelling and the location of the “valid probes” are presented in table 1.

Table 1: "valid" probes for tests n°2 and 15 (layout on figure 3)

Test n°2	TS3	TS7	TS8	TS9	TS10	TS19	TS20
x	30	40	50	50	50	80	100
y	0	0	5	0	0	0	0
z	0.7	1.4	1.4	0.7	1.4	1.4	1.4
Test n°15	TS1	TS3	TS5	TS7	TS11	TS12	TS16
x	30	40	40	50	80	80	100
y	0	3	-3	0	5	0	0
z	1.5	1.5	1.5	1.5	2	2	2

Figure 8 shows a typical velocity record by probe TS10 during release n°2 as function of time. Since the mean velocity evolves during the release, first because the flowrate decreases, but also because the wind is not steady (figure 2), it is necessary to choose a time integration slot sufficiently small as compared to these large scale time evolutions and sufficiently large as compared to the various turbulence time scales to analyse the structure of the locally stable jet. The former time scales are typically seconds or even tens of seconds. The latter are on the order of $L_{int}/U(x)$. Using the free jet approximation proposed by Khritov, $U(x)$ is about 30 m/s at 50 m from the release point and L_{int} is typically 5 m. Hence, the turbulent time scales are on the order of 0.1 s. As shown later during the discussion about the turbulence spectra, it was verified that the calculated flow properties (turbulence intensity, mean velocity) were reliable when the time slot varies between 1 s and 3 seconds. So, the signals were sampled in a series of about 1 s slots and, in each slot, the flow properties were calculated.

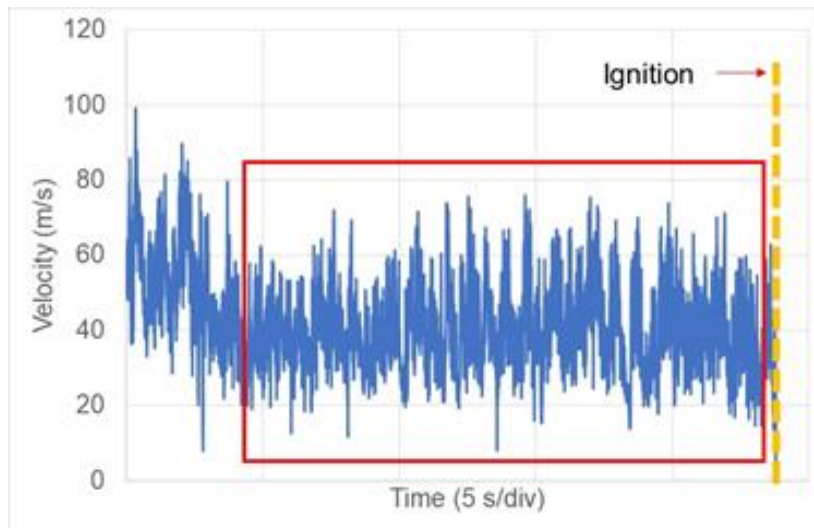


Fig. 8. velocity data of probes TS10 (test n°2). The red frame indicates the part of the record which was processed

4.2 Mean velocity and turbulence intensity

The evolution as function of time of the turbulence intensity and of the mean velocity are presented in Fig. 9 for test n°2. Even apparently reliable, some records may be questionable. Consider signal E2-3 (Test °2 sensor TS3) for instance where the turbulence intensity is much too large because the

mean velocity is too small (this sensor is the closest from the release point and its velocity signal should stand above the others). Possibly, the probe head of this sensor moved out from the axis of the jet.

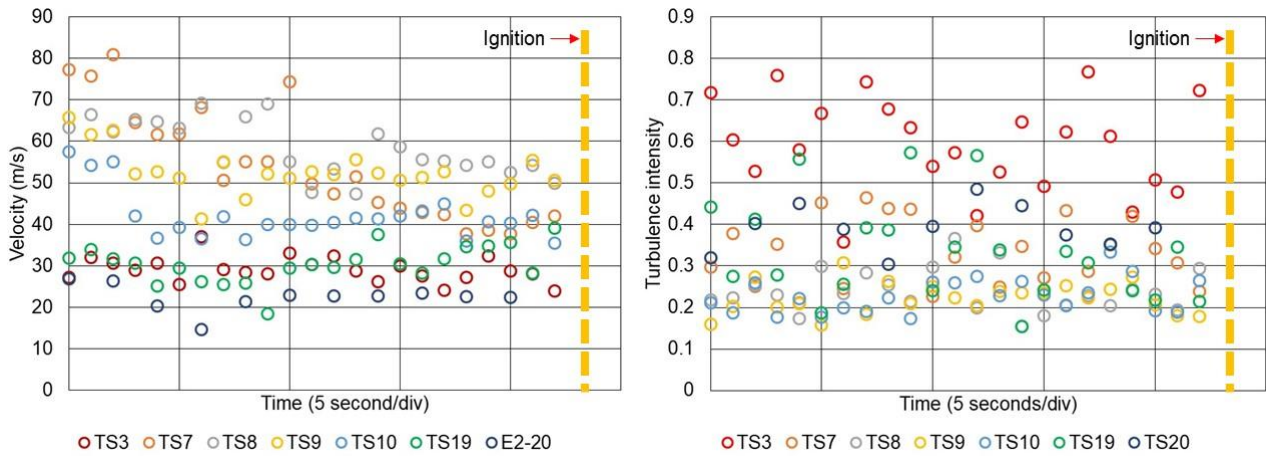


Fig. 9. Velocity and turbulence intensity averaged over 1 second length data bit for selected sensors of test n°2

Such aspects considered, the results can be compared to the existing jet theories (Fig. 10) for tests 2 and 15 (E2 and E15). The notional nozzle diameter is 570 mm (Birch, 1984) and the jet velocity is 400 m/s (sound speed).

There is a scattering in the mean velocity whereas the rms of the velocity fluctuations is more stable. This might be due to the lateral movement of the plume since, in jets, the variations on the mean velocity in the radial direction is much more pronounced than for the rms of the velocity fluctuations. The turbulence intensity is in line with the jet theories (free jets and wall jets). The variations of this parameter are due to the scattering of the mean velocity. Contrary to EXJET experimental series, the experimental points are clearly above the wall jet correlations. The best fit hyperbola is: $U_x/U_{exit} = 8.2/(x/D)$. This means that the outward horizontal spreading of the jet due to the presence of the wall does not compensate for the reduced half-space dispersion. Looking at the jet from the top and from the side (figure 11) reveals that the angles of the mixing layers are similar in the vertical plane and in the horizontal plane. This suggest that the first phenomenon (lateral outward increased expansion) is limited and that the jet behaves as a free jet expanding in a half space. This may be modeled using the free jet theory with a double flowrate or, similarly, using a double section for the flow. Doing this, the notional jet diameter should be multiplied by the square root of 2 in the free jet correlation. The reader could easily check that the experimental best fit correlation is retrieved.

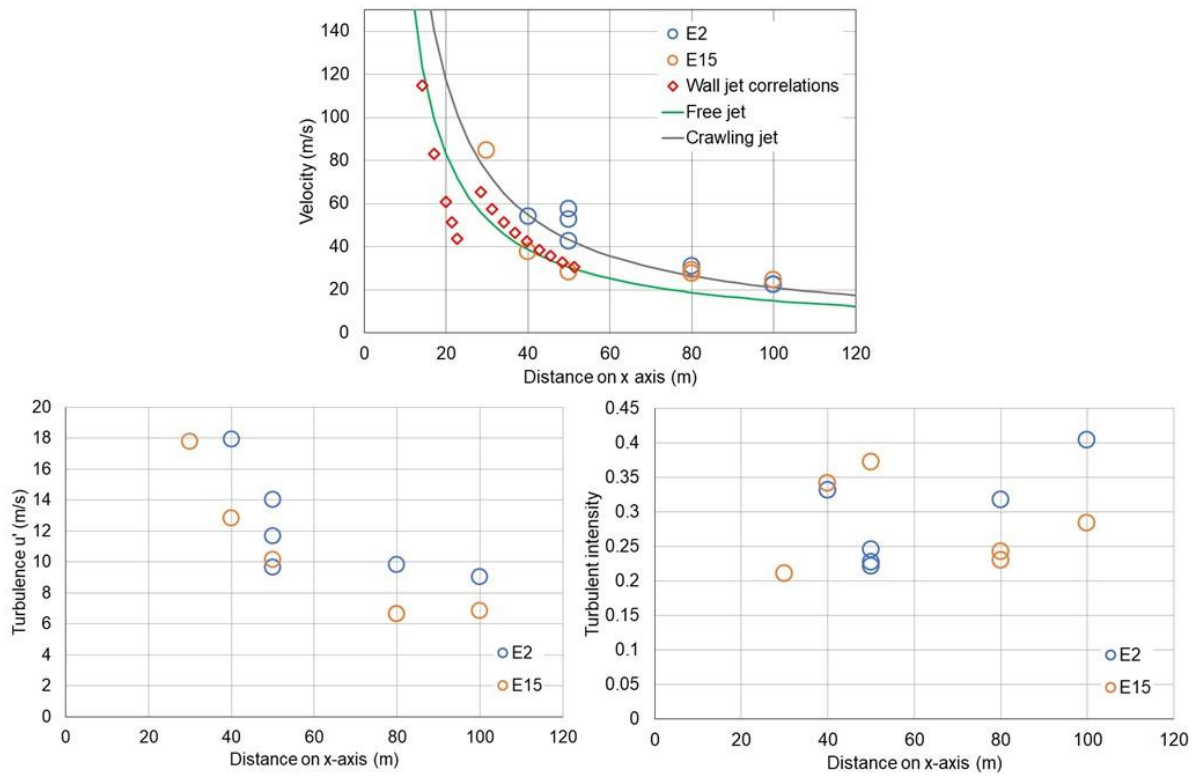


Fig. 10. Mean velocity, turbulence and turbulence intensity as function of the distance to the orifice.

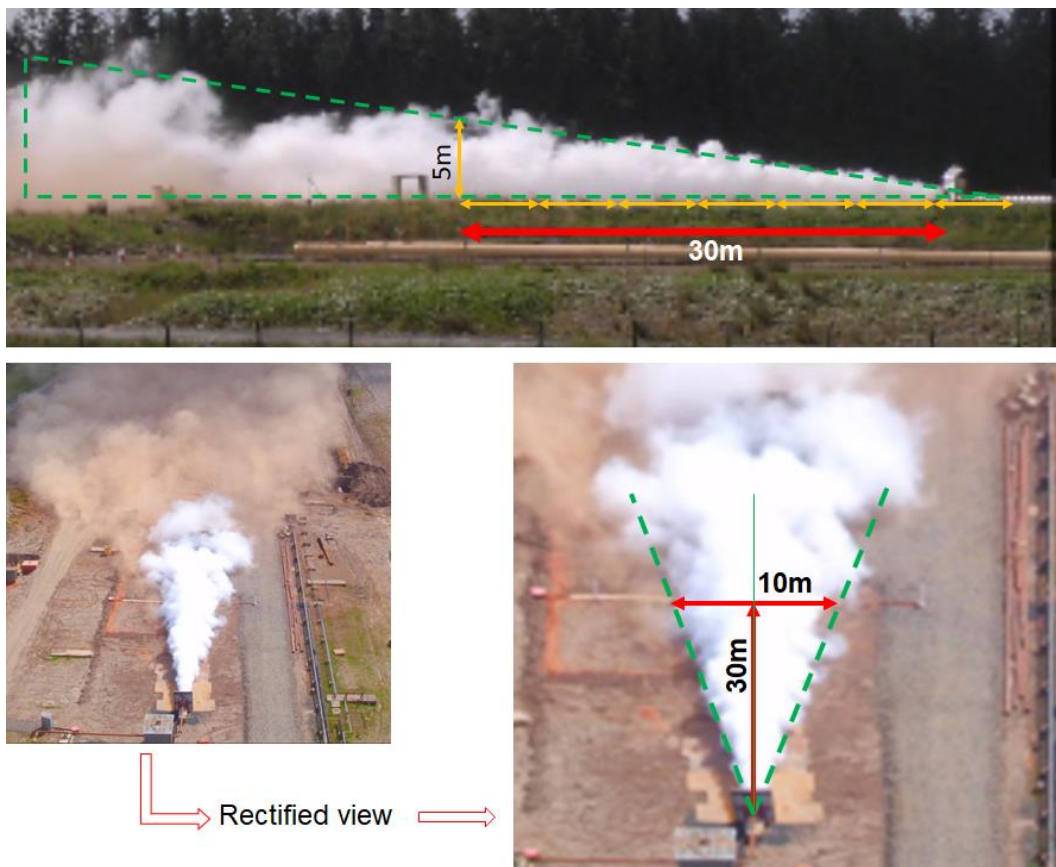


Fig. 11. Side view and top view (rectified to obtain orthogonal references) of AIRRE release. The vertical angle is about $8/9^\circ$ and the horizontal wide angle is about 18° (half angle 9°)

4.3 Integral scale and spectral energy of the turbulence

Assuming the turbulence field is fully developed and stable within the selected time slot (fig. 8), the autocorrelation curve should not change with time provided the duration over which the correlation curve is calculated is larger than the integral time of the turbulence. As explained before the latter is on the order of 0.1 s. The integration time for the autocorrelation time should at least be ten times larger. Once the latter is chosen, the time slot available for the data analysis is divided into N intervals of duration equal to the chosen integration time. The autocorrelation curve is calculated for each interval and the final autocorrelation curve is the average of N raw autocorrelation curves. This procedure, (which is based on Bartlett method: Bartlett M. S., 1948), provides a better accuracy in the correlation process especially when most of the information of the correlation is available in short time scales (typically 0.1 second in the present case). The important point is to choose adequately the integration time.

The influence of the integration time on the final correlation curve is shown on figure 12 left. Clearly the autocorrelation curves look very similar once the integration time is about 1 second. When it is smaller, probably part of the largest structures of the turbulence are lost, the autocorrelation signal changes significantly. When it is much larger (over 3 seconds), noise appearing at large time delays where normally the signals should not be correlated is integrated over all the curve due to the autocorrelation process smearing out the curve and introducing a baseline shift. A more quantitative estimate of the potential influence of the integration time is obtained looking at the integral time of the turbulence, L_t , which is the area under the autocorrelation curve. The evolution of L_t as function of the integration time is shown on figure 12 right. The latter reaches a sort of plateau in the region of 2 s and for larger values seem to diverge due to the integration of the noise. Following, in analyzing the data, the “measuring” time of about 1 s was chosen for all the transducers.

Considering the autocorrelation curve (1.25 or 2 s integration time slot), it is known (Hinze, 1975) that for large Reynolds number flows (fully developed turbulence), as in the present experimental situation, the curve should obey an exponential law: $R(t)=\exp(-t/L_t)$. In the present situation, this baseline exponential decay exists but superimposed on it is a low frequency sinusoidal signal (few Hz). This specificity is addressed later.

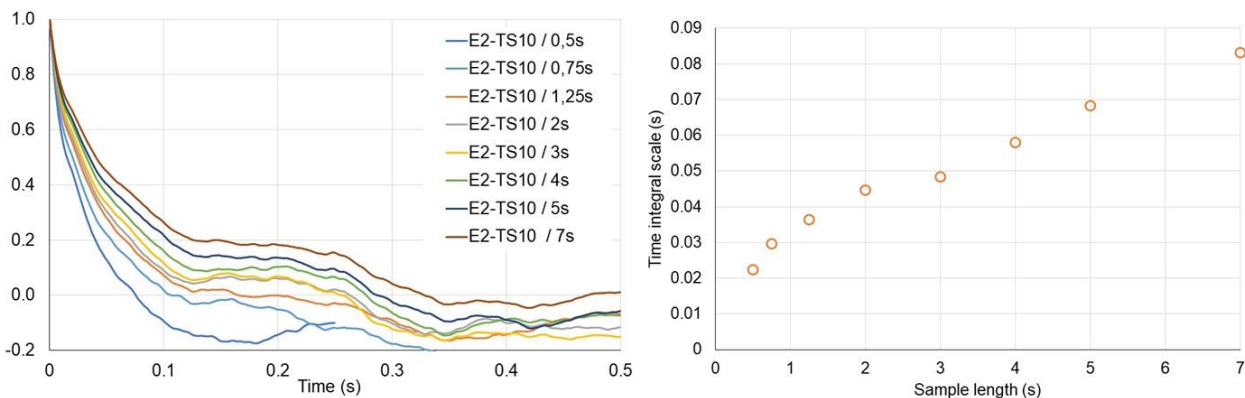


Fig. 12. Influence of the integration time on the autocorrelation curve (left) and on the integral time of the turbulence L_t (right)

The other autocorrelation curves are shown on figure 13 for tests n°2 and 15. The same features as described above are retrieved.

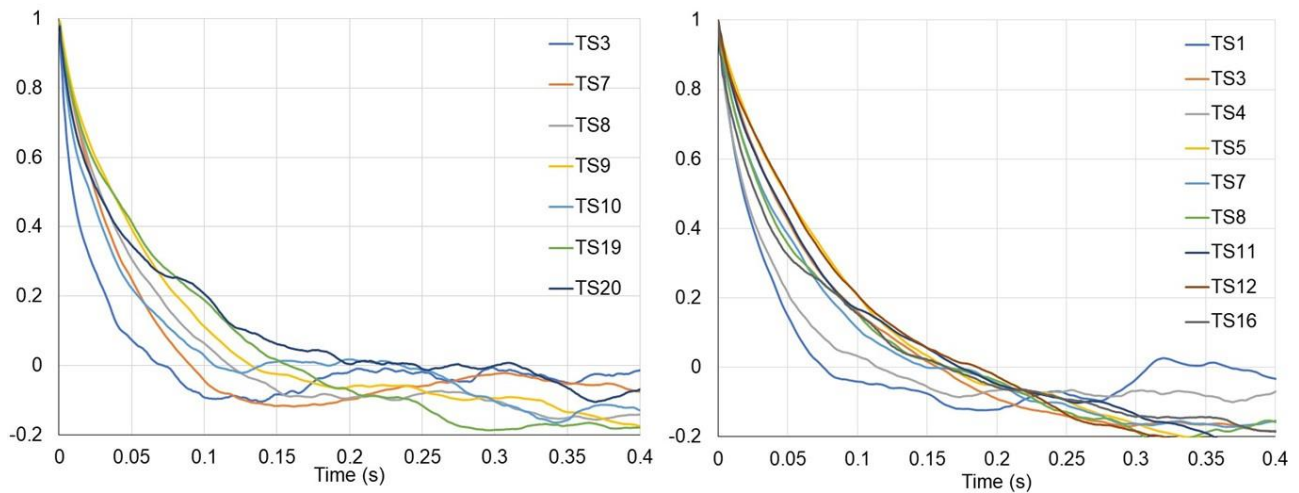


Fig. 13. Time auto-correlation curves obtained for test n°2 and 15 and various sensors.

The integral times of the turbulence are calculated and the integral scale are deduced using the Taylor assumption (Figure 14: $L_{int} = L_t \cdot \bar{U}$). It seems that the turbulence scales fit with the free jet theory down to 60 m from the release point and that, further downstream, a significant discrepancy appears. The scales drop to about 1 m or less and do not seem to change with distance anymore. Note this would be coherent with the turbulent scale of a flow along a wall knowing the transducers are located 1.5 m above ground (the integral scale of the turbulence at a distance h from the wall is h/2).

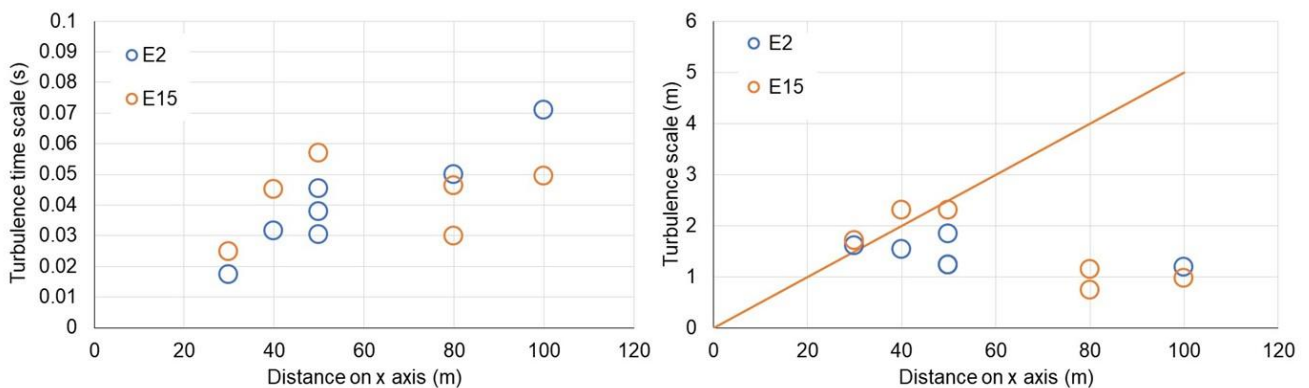


Fig. 14. Turbulent time scale L_t and integral turbulent scale L_{int} according to distance on x axis. The solid line corresponds to the standard free jet correlation

To go further, the turbulence energy spectra can be extracted from the Fourier transform of the autocorrelation curve and by applying the Taylor assumption to switch from the frequency space to the wavenumber space. The experimental distribution obtained for tests n°2 and 15 are shown on figure 15 (full lines) and compared to the free jet theory (dotted lines). The experimental signal fades for wavelengths on the order of 50 m^{-1} meaning a corresponding frequency of a few hundreds of Hz. This is the cutoff frequency of the pressure transducers. The slope of the turbulent cascade is in line with the Kolmogorov theory but the position of the spectra according to the wavenumber coordinate does not correspond to that of the free jet theory. Another difference is that a bump is visible at low wavenumbers, approximately at 0.3 m^{-1} . The corresponding wavelength is roughly 20 m and the corresponding duration (at 50 m from the release point so, close to sensor T10) amounts 0.3s which is the period of the sinusoidal wave superimposed on the exponential decay on the autocorrelation curve of figure 12. It can easily be shown, using the definition of the turbulence spectrum

superimposing a cosine function over the traditional exponential decay, that the resulting spectrum resembles those shown on figure 15, with the appearance of the bump, the displacement of the curve towards larger wavenumbers and a drop of the horizontal plateau.

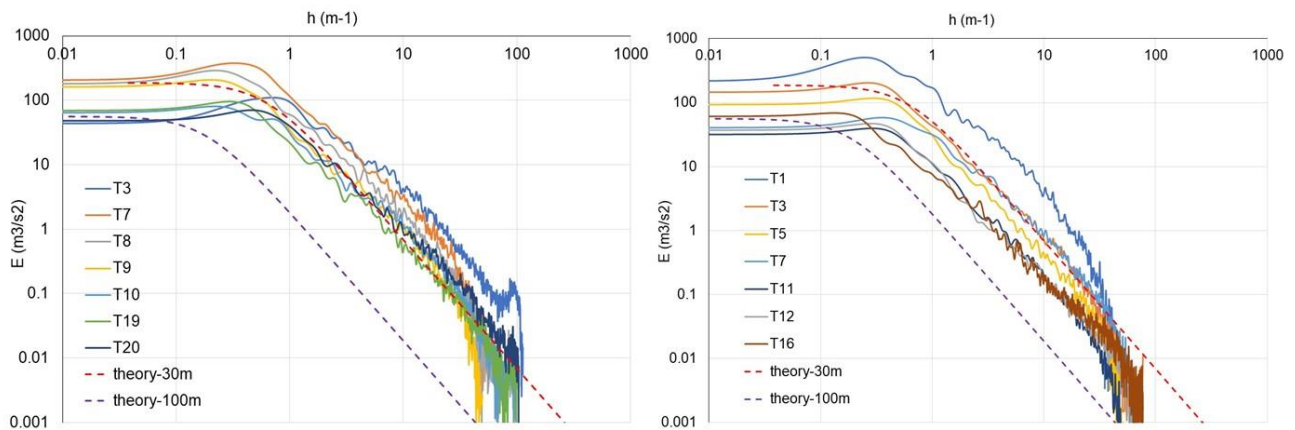


Fig. 15. Turbulence energy spectra for tests n°2 and 15 (dotted lines: free jet theory)

This large dynamic phenomenon seems to have a significant influence on the turbulence cascade. Note, it does not appear at small scale (EXJET). It might be visible on the videos under the form of large waves affecting the visible border of the cloud (figure 1). It could be a Kelvin-Helmholtz instability.

Conclusion

Perhaps for the first time, a very large scale under expanded gaseous jet was instrumented with turbulence probes. Free releases of pressurized natural gas performed during the AIRRE project were investigated. The release, under 100 bar and through a 100 mm orifice, was horizontal 1.5 m above the ground. The measuring technique is presented in this paper. It was carefully validated before the implementation of the field. The axial mean velocity, the turbulent velocity fluctuations, the integral scale of the turbulence and the spectra of the turbulence were obtained. The results are compared to tests at a smaller scale (12 mm orifice size).

Whereas small scale jets obey the wall jet theory, large scale jets do not. At least up to 60 m from the release point, the free jet theory would much better fit (apart the mixing occurs only in a half space). At large scale only, large scale pseudo periodic waves appear and interact significantly with the structure of the jet.

The proposed instrumentation proved to be sufficiently robust and can be used to interpret the results of the other tests of the AIRRE program.

References

- Abrahamsson H., Johansson B., Löfdahl L. (1996), An Investigation of the Turbulence Field in a Three-Dimensional Wall Jet, *Advances in Turbulence VI. Fluid Mechanics and its Applications*, vol 36. Springer, Dordrecht
- Bartlett M. S. (1948), Smoothing Periodograms from Times Series with Continuous Spectra, *Nature (London)*, Vol. 161, pp 686-687
- Birch A.D, Brown D.R., Dodson M.G., Swafield F. (1984), The structure and concentration decay of high-pressure jets of natural gas, *Comb. Sci. and Techno.*, vol. 36, pp. 249-261

- Hansen, O. R., Gavelli, F., Davis, S. G., and Middha, P. (2013), Equivalent cloud methods used for explosion risk and consequence studies, *Journal of Loss Prevention in the Process Industries*, 26(3), pp 511–527
- Hinze J.O. (1975), *Turbulence*, Mc GrawHill, New-York
- Hisken H., Mauri L., Atanga G., Lucas M., Van Wingerden K., Skjold T., Quillatre P., Dutertre A., Marteau T., Pekalski A., Jenney L., Allason D., Johnson M., Leprette E., Jamois D. (2020), Assessing the influence of real releases on explosions: selected results from large-scale experiments, 13th International Symposium on Hazards, Prevention, and Mitigation of Industrial Explosions Braunschweig, Germany
- Hussein H. J., Capp S. P., George W. K. (1994), Velocity measurements in a high-Reynolds-number, momentum-conserving, axisymmetric, turbulent jet, *J. Fluid Mech.*, vol 258, pp. 31-75
- Khritov K., M. Lyubimov D. A., Maslov V. P., Mineev B. I., Secundov A. N., Birch S. F. (2002), Three-dimensional wall jets - Experiment, theory and application, 40th AIAA Aerospace Sciences meeting and exhibit
- Launder B. E., Rodi W. (1983), The turbulent wall jet -measurements and modeling, *Annual Review of Fluid Mechanic*
- Mc Caffrey B. J., Heskestad G. (1976), A robust bidirectional low-velocity probe for flame and fire application, *Combustion and Flame*, vol. 26, pp125-127
- Proust, C., Jamois D. (2020), Measuring the flow and the turbulence in dust air mixtures and in flames using a modified Mc Caffrey gauge. To be published
- Sun H. (2002), The Development of Three-dimensional Wall Jet, Thesis, Mc Master University
- Tamanini F. (1990), Turbulence effect on dust explosion venting, *Plant/Opération Progress*, vol. 9
- Tamanini F., Chaffee J. L. (1991), Turbulent unvented gas explosions under dynamic mixture injection conditions, 23rd Symp (Int.) on Combustion, The Combustion Institute, Pittsburgh pp. 851-858
- Skjold, T., Hisken H., Mauri L., Atanga G., Bernard L., Van Wingerden K., Foissac A., Quillatre P., Blanchetiere V., Dutertre A., Kostopoulos D., Pekalski A., Allason D., Johnson M., Jenney L., Leprette E., Jamois D. (2018), Assessing the influence of real releases on explosions: motivation and previous work, *Proceedings of the Twelfth International Symposium on Hazards, Prevention and Mitigation of Industrial Explosions (12 ISHPMIE)*, Kansas City, 12-17 August 2018: 24 pp. Fike Corporation, Blue Springs, MO, USA.